TECHNICAL REPORT No. 18

TO

STRETCH FORMING AND FRACTURE
OF STRONGLY TEXTURED Ti ALLOY SHEET

K. S. CHAN* AND D. A. KOSS

DEPARTMENT OF METALLURGICAL ENGINEERING
MICHIGAN TECHNOLOGICAL UNIVERSITY
HOUGHTON, MICHIGAN U.S.A.

*CURRENTLY: DEPARTMENT OF MATERIALS SCIENCE
             AND ENGINEERING
             STANFORD UNIVERSITY
             STANFORD, CA

DTIC
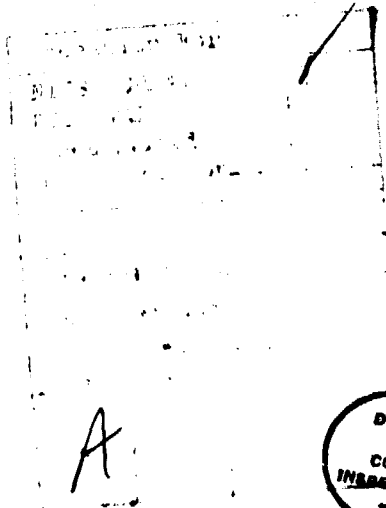ELECTE
JUN 1 0 1982
S
A
D

82 06 10 040

REPORT DOCUMENTATION PAGE	READ INSTRUCTIONS BEFORE COMPLETING FORM

1. REPORT NUMBER	2. GOVT ACCESSION NO.	3. RECIPIENT'S CATALOG NUMBER
No. 18	AD-A115 385	

4. TITLE (and Subtitle)	5. TYPE OF REPORT & PERIOD COVERED
STRETCH FORMING AND FRACTURE OF STRONGLY TEXTURED Ti ALLOY SHEET	
	6. PERFORMING ORG. REPORT NUMBER

7. AUTHOR(s)	8. CONTRACT OR GRANT NUMBER(s)
K. S. Chan and D. A. Koss	N00014-76-C-0037, NR 031-756

9. PERFORMING ORGANIZATION NAME AND ADDRESS	10. PROGRAM ELEMENT, PROJECT, TASK AREA & WORK UNIT NUMBERS
Department of Metallurgical Engineering Michigan Technological University Houghton, MI 49931	

11. CONTROLLING OFFICE NAME AND ADDRESS	12. REPORT DATE
Office of Naval Research 800 N. Quincy Street Arlington, VA 22217	March 1982
	13. NUMBER OF PAGES
	19

14. MONITORING AGENCY NAME & ADDRESS(if different from Controlling Office)	15. SECURITY CLASS. (of this report)
	Unclassified
	15a. DECLASSIFICATION/DOWNGRADING SCHEDULE

16. DISTRIBUTION STATEMENT (of this Report)

Distribution of this document is unlimited.

17. DISTRIBUTION STATEMENT (of the abstract entered in Block 20, if different from Report)

18. SUPPLEMENTARY NOTES

19. KEY WORDS (Continue on reverse side if necessary and identify by block number)

Stretch forming, plastic anisotropy, Ti-6Al-4V, Ti-5Al-2.5Sn, Fracture, Sheet metal deformation.

20. ABSTRACT (Continue on reverse side if necessary and identify by block number)

The influence of plastic anisotropy and R-value on the stretch forming and fracture behavior of strongly textured Ti-6Al-4V and Ti-5Al-2.5Sn sheet has been examined utilizing sheet specimens with a wide range of R-values but with similar work hardening and strain rate sensitivity characteristics. The results indicate that a high R-value and difficult through-thickness slip enhance the forming limit as well as fracture strains when the minor strain in the plane of the sheet is negative, this affect being most pronounced

DD FORM 1473 EDITION OF 1 NOV 65 IS OBSOLETE
S/N 0102-014-6601

(cont'd)

20. Abstract (cont'd)

at uniaxial tension. At plane strain, the R-value has little or no influence on the limit or fracture strain. A direct determination of the effect of R-value on the biaxial stretch forming characteristics of Ti-6-4 sheet is precluded by the intervention of fracture prior to localized necking when the minor strain is positive. The influence of plastic anisotropy on both the localized necking and the fracture behavior can be generally understood in terms of difficulty of attaining critical thickness strains as through-thickness slip becomes more difficult.

STRETCH FORMING AND FRACTURE

OF STRONGLY TEXTURED Ti ALLOY SHEET

K. S. Chan* and D. A. Koss
Department of Metallurgical Engineering
Michigan Technological University
Houghton, Michigan 49931

ABSTRACT

The influence of plastic anisotropy and R-value on the stretch forming
and fracture behavior of strongly textured Ti-6Aℓ-4V and Ti-5Aℓ-2.5Sn sheet
has been examined utilizing sheet specimens with a wide range of R-values
but with similar work hardening and strain rate sensitivity characteristics.
The results indicate that a high R-value and difficult through-thickness slip
enhance the forming limit as well as fracture strains when the minor strain
in the plane of the sheet is negative, this effect being most pronounced at
uniaxial tension. At plane strain, the R-value has little or no influence
on the limit or fracture strain. A direct determination of the effect of
R-value on the biaxial stretch forming characteristics of Ti-6-4 sheet is
precluded by the intervention of fracture prior to localized necking when
the minor strain is positive. The influence of plastic anisotropy on both
the localized necking and the fracture behavior can be generally understood
in terms of difficulty of attaining critical thickness strains as through-
thickness slip becomes more difficult.

*Currently at the Department of Material Science and Engineering,
Stanford University, Stanford, CA 94305.

INTRODUCTION

The strong influence of crystallographic texture and plastic anisotropy on deep drawing is well established. However, in stretch forming operations the effects of work hardening and strain rate hardening clearly dominate, and plastic anisotropy is usually considered to be a minor factor (see refs. 1, 2 for reviews). This is understandable for fcc and bcc alloys where minor changes of the strain or strain rate hardening can dominate the effects of plastic anisotropy which, due to the crystallography of slip in fcc/bcc metals, are probably relatively small. As a result, interpretations of the existing data which relate stretch forming and plastic anisotropy have been conflictive.[1,2-5] On the other hand, the effects of plastic anisotropy on localized necking can be quite pronounced in strongly textured hcp alloys. In a separate study, we have observed that large variations of plastic anisotropy affected through the control of crystallographic texture in α(hcp)-β(bcc) Ti alloys can increase significantly the limit strain as well as the fracture strain in <u>uniaxial</u> tension.[6] Using the R-value as a measure of plastic anisotropy (R is the ratio of the width to thickness strain in a tension test), this investigation examines the influence of crystallographic texture and R-value on the biaxial <u>stretch forming</u> behavior of strongly textured Ti alloy sheet. The previous study of the stretchability of α-β Ti alloys has been based on material exhibiting a small range of R-values (R = 0.6 - 1.0).[7] In those cases where Ti alloy sheet with a high degree of plastic anisotropy has been examined, the studies have been confined to observations of biaxial strengthening or the relationships between texture and R-value.[8-12] This study presents forming limit diagrams for Ti-6Aℓ-4V and Ti-5Aℓ-2.5Sn sheet with either a strong basal or a strong basal-transverse texture. The large variation of plastic anisotropy ($0.5 \leq R \leq 12$) at relatively constant strain and strain rate hardening rates in these materials permits a more direct evaluation of through-thickness slip and the R-value on both the localized necking and the fracture behavior under stretch forming conditions.

EXPERIMENTAL

The material used in this study is identical to that in which the uniaxial tensile properties were examined.[6] As described,[6] the 1.4mm Ti-6Aℓ-4V (Ti-6-4) and Ti-5Aℓ-2.5Sn (Ti-5-2.5) thick sheet was processed to possess either a strong basal texture (R = 12) or a basal-transverse texture (R = 0.5 to 2.0). The Ti-6-4 sheet possesses an equiaxed α-β microstructure (see Fig. 1 of ref. 2) with a grain size 10μ while the Ti-5-2.5 alloy is primarily α-phase of grain size 14μ. Crystallographic textures are shown in Fig. 2 of ref. 6.

Table I summarizes the uniaxial tensile properties of the Ti-6-4 and Ti-5-2.5 sheet studied in this investigation. As indicated in Table I, the textured Ti alloy sheet exhibits relatively constant n and m values (n $\simeq$ .05, m $\simeq$ .014) but a wide variation of R-values ranging from R = 0.5 to R = 12.

In a manner similar to that used by Hecker,[13] punch stretch testing of Ti alloy sheet has been performed on a Baldwin universal testing machine equipped with a rigid hemispherical punch of 50.8mm diameter. The specimens were photo-gridded with 1.27mm diameter contacting circles which permit the measurement of the major and minor principal strains (ε_1 and ε_2 respectively) in the plane of the sheet. As in Hecker's procedure,[13] the degree of biaxiality of the strain path was controlled by testing strip specimens of varying width and by varying the lubrication, 0.4mm teflon sheets with silicone grease in this case, between the punch and sheet specimen. Uniaxial tensile tests of narrow as well as wide strip specimens were also performed.

The forming limit curves have been constructed based on the criterion proposed by Hecker,[13] which considers the strain just outside a visual localized neck as the forming limit strain. In tests in which necking was not readily evident, careful examination at magnifications up to 50X were conducted to determine if fracture occurred prior to the onset of localized necking. In the case of fracture, the major principal fracture strain ε_{1f} has been measured

indirectly. The thickness strain at fracture ε_{3f} and the minor surface strain at fracture ε_{2f} both can be obtained directly (one from thickness measurements and the other from grid determinations at the edge of fracture surface). The maximum principal fracture strain ε_{1f} can then be calculated from the expression $\varepsilon_{1f} + \varepsilon_{2f} + \varepsilon_{3f} = 0$.

RESULTS

The forming limit diagrams (FLD) of basal textured Ti-6-4 and Ti-5-2.5 sheet are shown in Fig. 1 and Fig. 2 respectively. The FLD's of basal textured Ti-6-4 and Ti-5-2.5 sheet with R = 12 are characterized by a large negative minor strain regime ($\varepsilon_2 < 0$) but a relatively small positive minor strain region ($\varepsilon_2 > 0$); see Figs. 1 and 2. In all cases, the magnitudes of the neck-free strain, necked strain and the fracture-affected strains are very similar to each other. In addition, the fracture strains are also just slightly above the forming limit curve. Careful examination (at magnifications up to 50X) of test specimens stretched under balanced biaxial conditions indicates that fracture appears to have intervened prior to any visible localized necking. At plane strain, localized necking is just visible but is readily evident in uniaxial tension. Thus we conclude that the high R-value Ti-6-4 and Ti-5-2.5 sheet fails by localized necking in the $\varepsilon_2 < 0$ region but fracture in the biaxial tension region ($\varepsilon_2 > 0$). It should also be noted that, given their similar n, m, and R-values, the basal-textured Ti-6-4 and Ti-5-2.5 alloys exhibit FLD's which are identical within experimental error; compare Figs. 1 and 2.

The FLD's for the basal-transverse material (R ≃ 1), shown in Fig. 3, are a distinct contrast to those for the basal texture (R ≈ 12) material shown in Figs. 1 and 2. Whether the localized neck forms perpendicular to the TD (Fig. 3a) or to the RD (Fig. 3b),* the limit strains and fracture strains in the negative

_____

*In the punch-stretch testing of full width sheet specimens with the basal-transverse texture, localized necking occurs exclusively normal to the TD. Thus, the balanced biaxial limit strains for localized necking normal to the RD could not be determined.
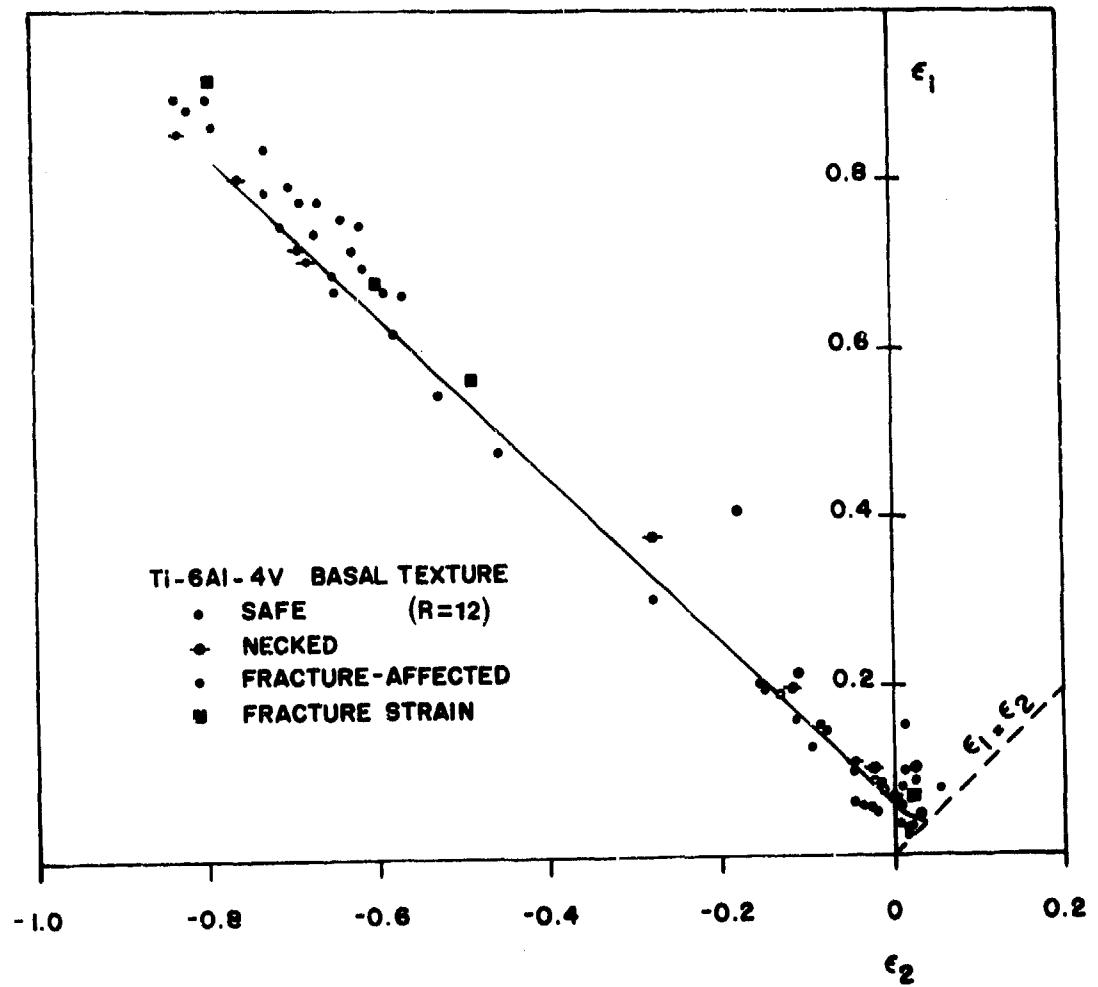
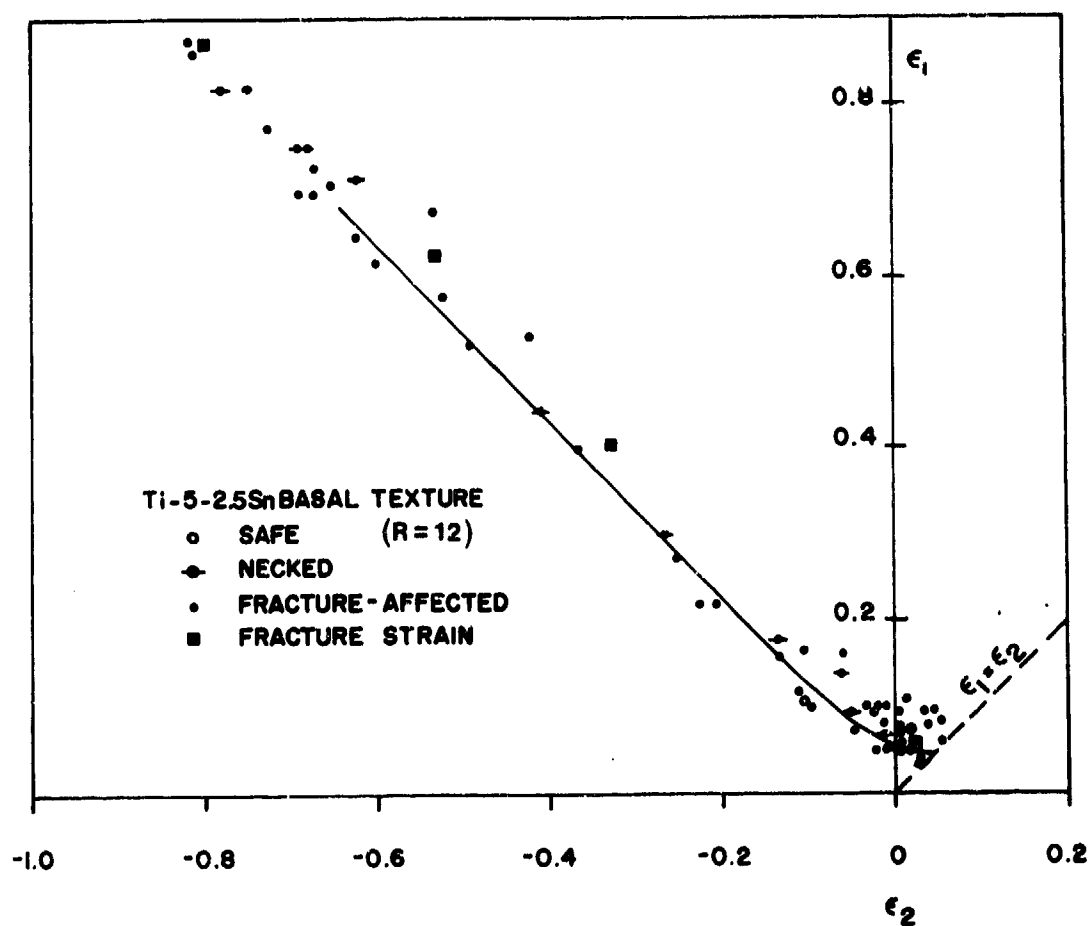Fig. 1. A forming limit diagram for Ti-6Aℓ-4V sheet with a strong basal
texture and R = 12.

Fig. 2. A forming limit diagram for Ti-5Aℓ-2.5Sn sheet with a strong basal texture and R = 12.
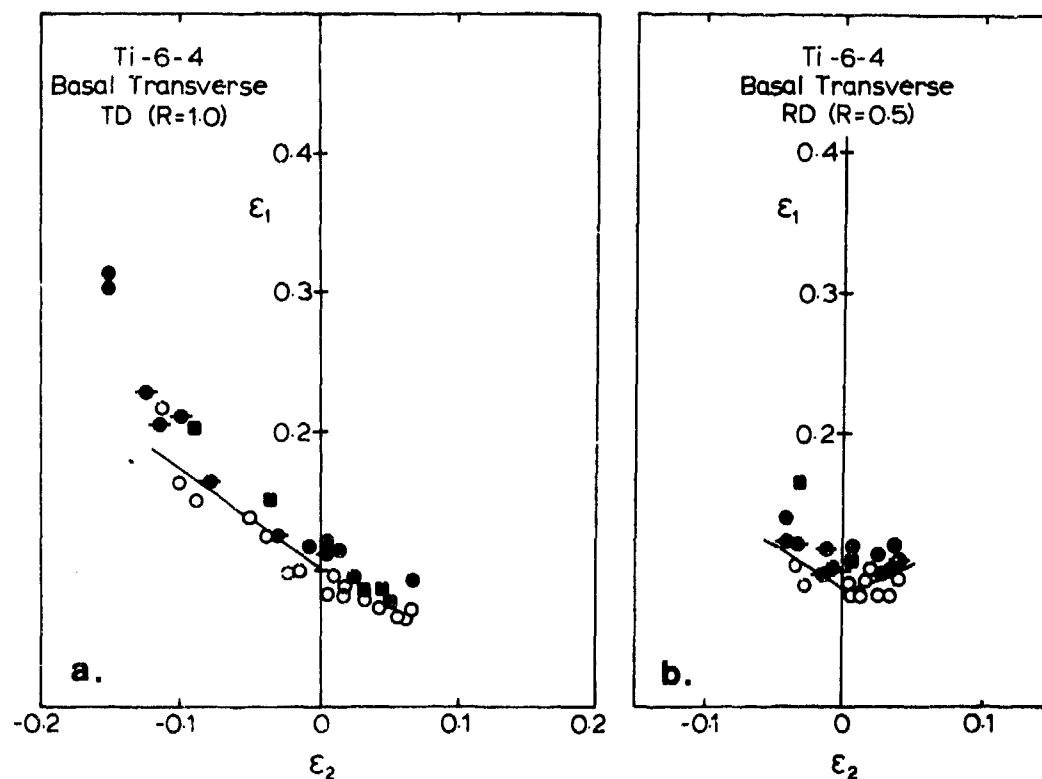
Fig. 3. Forming limit diagrams for Ti-6Al-4V sheet with a basal-transverse texture with localized necking occurring: (a) normal to the transverse direction and (b) normal to the rolling direction.

minor strain region, especially near uniaxial tension, are much smaller than
those in Figs. 1 and 2.

Figure 4 compares the FLD's obtained in the present study and those for
Ti-6-4 sheet with a weak texture and small R-value[7] as well as CP-Ti sheet with
a moderate R-value.[14] Despite the differences in textures, the Ti-6-4 specimens
possess similar strain hardening and strain rate sensitivity characteristics
$(n = .05 - .06$ and $m = .012 - .016)$. Thus, a comparison of the results as
summarized in Fig. 4 indicates that a high R-value $(R = 12)$ enhances the forming
limit (limit strain to localized necking) in the negative minor strain $(\varepsilon_2 < 0)$
of the FLD.

In the biaxial stretching region of the FLD $(\varepsilon_2 > 0)$, the basal and the
basal-transverse textured materials fracture prior to localized necking. Thus,
the effect of the R-value on localized necking in the $\varepsilon_2 > 0$ region cannot be
directly established. However, a comparison of the results of the CP-Ti and
the weakly textured Ti-6-4, both of which failed by localized necking even in
the $\varepsilon_2 > 0$ region, reveals that these materials have comparable stretch forma-
bility in the $\varepsilon_2 > 0$ region despite the lower n and m values of the Ti-6-4
material. It is well known that high n and m values enhance stretch formability.
Thus, the similarity in limit strains between CP-Ti and Ti-6-4 suggests the
likelihood that a high R-value decreases the forming limit strain in the $\varepsilon_2 < 0$
region.

Fractographic studies indicate that the fracture of textured Ti alloy sheet
at uniaxial tension as well as under biaxial tension occurs by a ductile fracture
process. In the basal textured Ti-6-4 and Ti-5-2.5 sheet, the fracture surfaces
are characterized by large, deep dimples at uniaxial tension but much more shallow
and small dimples under biaxial tension. Figure 5 shows typical fracture surfaces
of the basal textured Ti-6-4; the Ti-5-2.5 was identical in appearance despite the
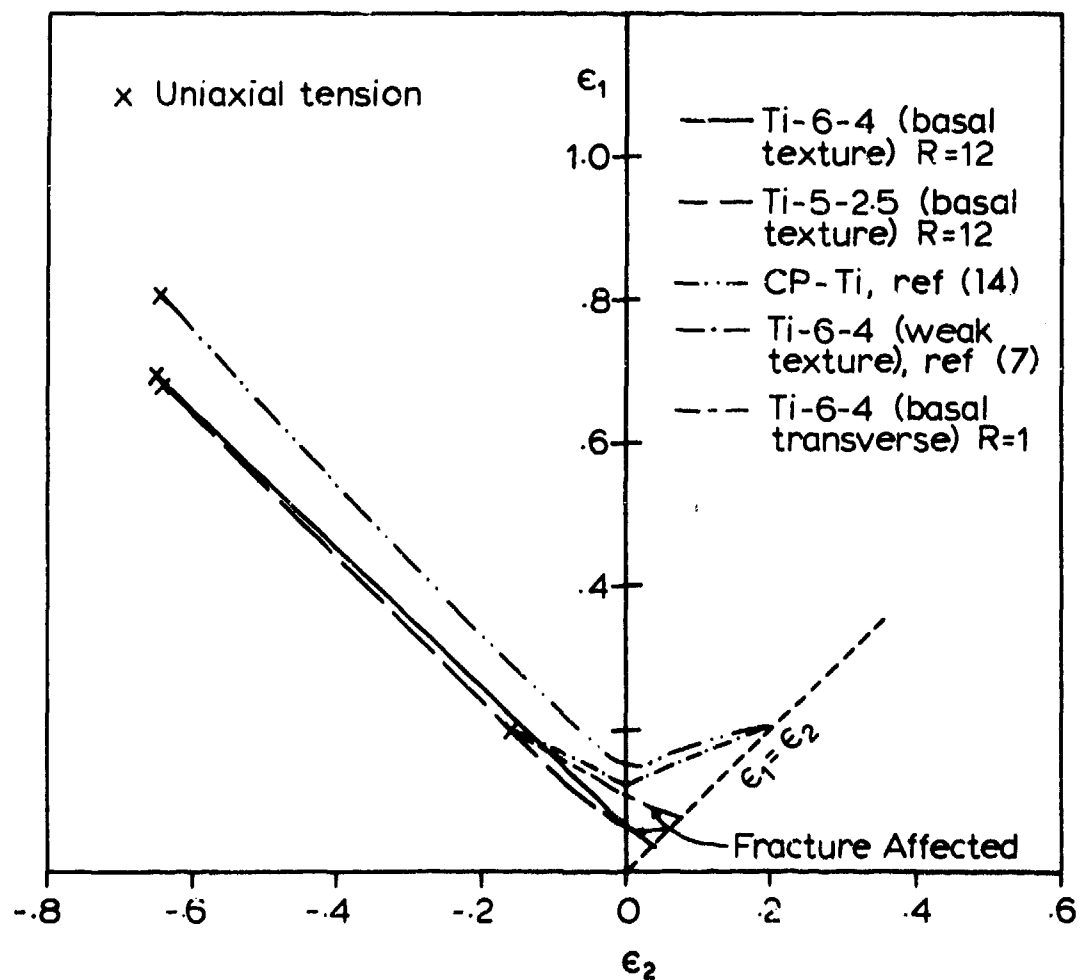near-absence of the β-phase. These results are consistent with good ductility in

Fig. 4. A comparison for forming limit diagrams for Ti-6Aℓ-4V, Ti-5Aℓ-2.5Sn and commercially pure Ti sheet.
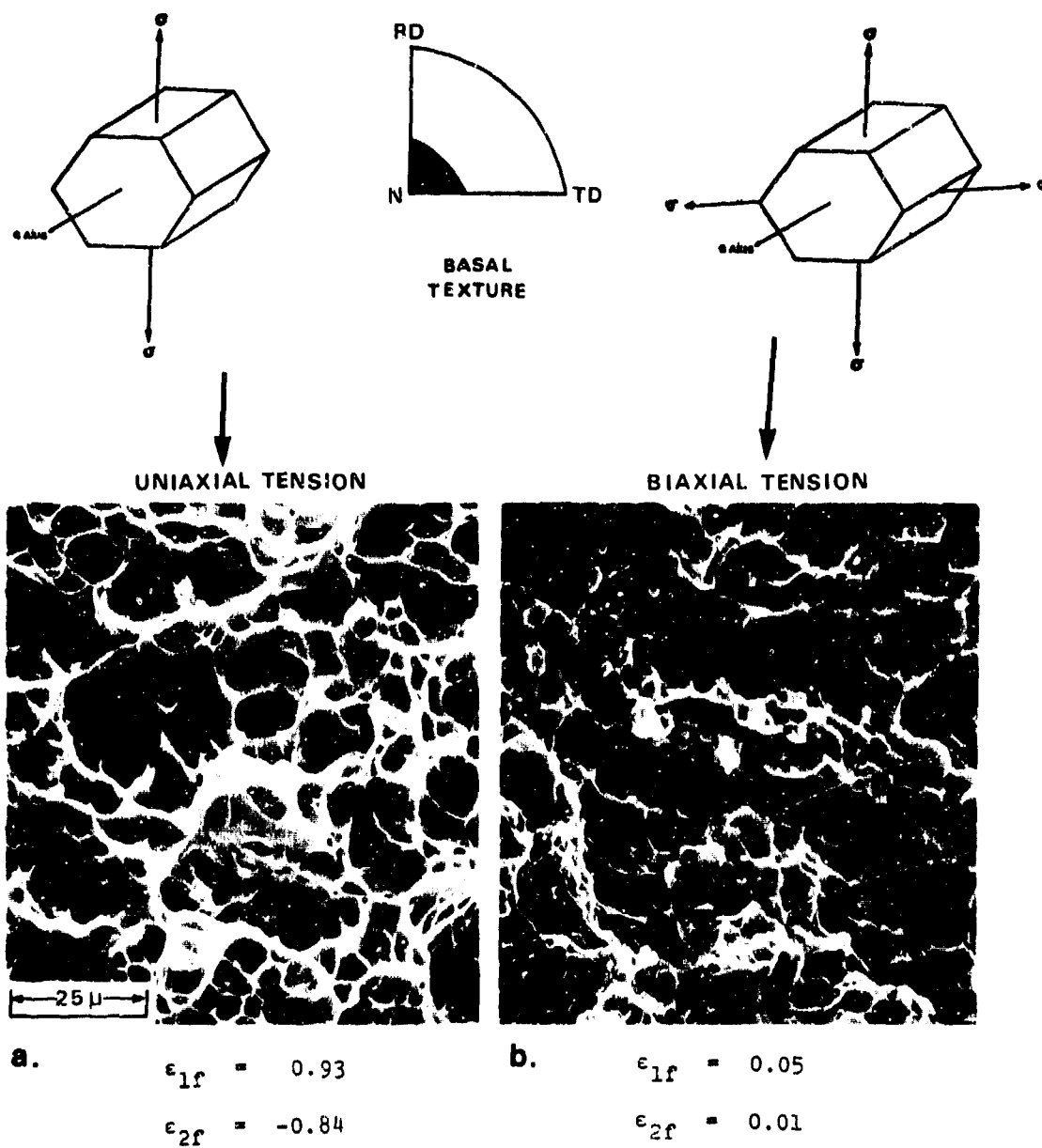
Fig. 5. Scanning electron micrographs showing the fracture surfaces of Ti-6Aℓ-4V sheet with a strong basal texture tested in: (a) simple tension and (b) balanced biaxial tension.

uniaxial tension but inferior ductility in biaxial tension. The basal-transverse texture material also exhibits smaller, more shallow dimples if one compares biaxial behavior to that in uniaxial. However, the differences in features are not as marked as in Fig. 5 which is consistent with the smaller differences in failure strains between uniaxial vs. biaxial deformation in Fig. 1 vs. Fig. 3.

DISCUSSION

(a) Forming Limit Diagrams and Localized Necking

That an increase in the R-value increases the limit strain in the negative minor strain ($\epsilon_2 < 0$) region of the FLD can be understood in terms of the behavior in uniaxial tension.[6] Applying the Marciniak-Kuczynski (M-K) analysis,[15] we assume that an initial imperfection or inhomogeneity exists in the original material and that it is the development of this imperfection which causes localized necking. If the imperfection exits along or near a direction of zero extension, it is at least near plane strain initially, and stress-path hardening should be minimal. However, the behavior in uniaxial tension indicates that localized necking of strongly textured Ti alloy sheet occurs at approximately a constant value of the thickness strain ($\epsilon_3 = \epsilon_3^*$) which is independent of the R-value.[6] These experimental results are supported by calculations by Chan, Koss, and Ghosh who extend the M-K analysis and show that ϵ_3^* is indeed a constant value in the negative minor strain region of the FLD and is independent of R but depends, as expected, on the n and m values and material imperfection size.[16]

Applying a critical thickness strain ϵ_3^* criterion to the negative minor strain region of the FLD in Fig. 4, we anticipate three trends: (1) a large increase in limit strain with increasing R-value as uniaxial tension is approached, (2) a slope of $d\epsilon_1/d\epsilon_2 = -1$, and (3) little or no influence of R-value on plane strain behavior. Examination of Fig. 4 indicates all of these trends exist at least in the high or moderate R-value materials. The rationale for the first trend is discussed in detail elsewhere and reflects the increased difficulty of

attaining ϵ_3^* if through-thickness slip is difficult and the R-value is high. Trend (2), the slope, is a consequence of: $\epsilon_1 = -\epsilon_2-\epsilon_3^*$, where ϵ_3^* is a constant at fixed n and m values. The third trend is also satisfied by the observed behavior because there is no change in stress state during plane strain loading[17] and also $\epsilon_1 = -\epsilon_3$ when $\epsilon_2 = 0$. As a result, the major principal strain at localized necking ϵ_1^* equals the critical thickness strain ϵ_3^* at plane strain, and as concluded previously, ϵ_3^* is not affected by the R-value but depends on the n and m value and material imperfection. Thus ϵ_1^* is roughly a constant ($\epsilon_1^* = 0.8$) for the present investigation, $\epsilon_1^* = .12$ from ref. 7 and $\epsilon_1^* = .15$ for CP Ti.[14] It should be noted that the plane strain behavior is also consistent with the formability analysis of Neale and Chater[18] who demonstrate analytically an independence of plane strain limit strain on either the R-value or the choice of plastic constitutive law; their analysis is also based on no change of stress state during plane strain loading.

The experimental results in Fig. 4 also imply that if CP Ti had a reduced strain and strain rate hardening to match that of the Ti-6-4 with a weak texture, then the effect of R-value would be to <u>decrease</u> the limit strain in the biaxial tension region. Without resorting to considerable speculation, we wish only to note that this behavior can also be understood in terms of an imperfection analysis. As recognized by Marciniak, Kuczynski and Pokara[19] and by Sowerby and Duncan,[20] the influence of plastic anisotropy on localized necking in the biaxial region can be understood in terms of the shape of the yield or flow locus. The effect of increasing the R-value to values > 1 (assuming planar isotropy) is to extend the elliptical yield locus along the equal biaxial stress path $\sigma_1 = \sigma_2$). The result is a much reduced minor radius of the elliptical yield surface and less stress-path hardening between biaxial tension and plane strain. A consequence of the sharp curvature of the yield surface is that a high R-value material containing an imperfection and stretched in equal biaxial tension will locally attain the plane strain condition for localized necking at an earlier

stage of the straining process than that of a low R-value material.

In the punch stretching analysis of Wang and Wenner,[21] the effect of a large R-value is to increase the peak strain, cause a shift of the location of the strain peak and produce a more non-uniform strain distribution. In the present investigation, biaxial stretching of the textured Ti alloy sheet tends to produce deformation which is localized near the pole of the cup and fracture intervenes at low strain levels. As a result, accurate strain distribution measurements cannot be made and a direct determination of the effects of R-value on strain distribution is precluded.

(b) **Fracture Behavior**

Fracture of the strongly textured Ti alloy sheet is characterized by the pronounced effect of loading path on the fracture strains of, in particular, the material with high R-value. For example, the equivalent strain to fracture $\bar{\epsilon}_f$ at R = 12 is 0.79 in uniaxial tension but only 0.19 in biaxial tension. Thus, high R-value and difficult through-thickness slip is especially effective in increasing the fracture strains in uniaxial tension, while decreasing slightly the fracture strain at plane strain and in balanced biaxial tension. In all cases a ductile fracture process is observed involving void formation and coalescence (see Fig. 5) with the dimples formed in biaxial tension being smaller and more shallow. It is thus somewhat surprising that the fracture behavior described above and depicted in Figs. 1-3 can be predicted with roughly the same degree of success by two quite difference failure criteria.

LeRoy and Embury have suggested a macroscopic criterion for failure of sheet: that fracture occurs at a critical thickness strain ϵ_{3f}^{*}.[22] Given that the volume of material is roughly a constant even at fracture, (thus: $\epsilon_{1f} + \epsilon_{2f} + \epsilon_{3f}^{*} = 0$), this criterion implies:

$$\epsilon_{1f} = -\epsilon_{2f} - \epsilon_{3f}^{*} \tag{1}$$

where $-\varepsilon_{3f}^{*}$ = material constant and ε_{1f} and ε_{2f} are the major and minor strains at fracture. The value of ε_{3f}^{*} may be determined from a uniaxial tensile test and thus Equation (1) can be used to predict a fracture limit map which should be linear with a slope of $d\varepsilon_{1f}/d\varepsilon_{2f}$ = -1.

A much different approach to the ductile fracture of sheet has been taken by Ghosh who assumed that shear joining of voids after considerable void growth is the governing microstructural process.[23] Treating the probability of joining the voids by a shear process to be depending on a product of triaxial and shear stresses, Ghosh[23] arrives at essentially a stress-based failure criterion:

$$(1+\alpha)\ \sigma_{1f}^{2} = K_{cr} \tag{2}$$

where σ_{1f} is the maximum principal stress at fracture, α is the instantaneous stress ratio, and K_{cr} is the critical fracture-stress parameter, which is a material constant. Equation (2) may be evaluated from a uniaxial tension test in order to predict the major and minor principal strain ε_{1f} and ε_{2f} at fracture. It should be noted that this analysis assumes voids form at small strains at inclusions, which do not occur in Ti alloys since inclusions are not present. On the other hand, shear localization is quite pronounced in the two-dimensional modeling of tensile deformation near voids in Ti-6-4.[24]

Figure 6 shows a comparison between predicted fracture maps based on Equations (1) and (2) as compared to experimental observations. For material with a high R-value (note that the basal texture Ti-5-2.5 behavior is nearly identical to the Ti-6-4 in Fig. 6a), the calculated curves are nearly identical and in excellent agreement with the experimental data. The fracture strains in <u>uniaxial</u> tension at R = 12 are quite large because of the difficulty of through-thickness slip resulting in either: (a) a large equivalent strain $\bar{\varepsilon}$ at the critical ε_{3}^{*} or (b) a small σ_{1} at a given $\bar{\varepsilon}$ (stress criterion). Strain paths near balanced biaxial stress state simply result in the converse to that in uniaxial tension. A decrease of dimple size from uniaxial to biaxial tension
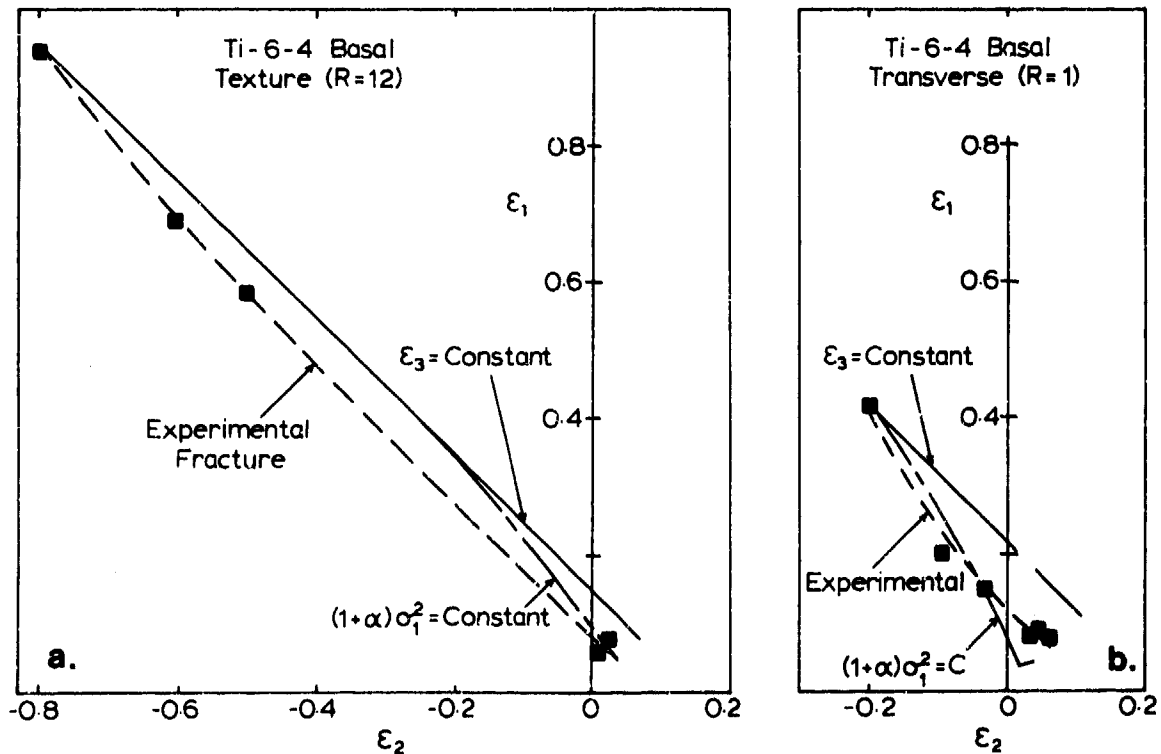
Fig. 6. Fracture limit diagrams for Ti-6Aℓ-4V sheet comparing the experimentally observed behavior to that predicted by two different fracture criteria. Data is for sheet with either: (a) a basal texture or (b) basal-transverse texture.

(see Fig. 5) also must be rationalized in terms of an enhanced shear linking of smaller voids due to larger triaxial stresses (stress criterion and the $(1+\alpha)$ term in Equation (2)).

Neither failure criterion predicts fully the fracture of the basal-transverse material; see Fig. 6b. The stress-based criterion is in reasonable agreement in the negative ε_2 region but badly underestimates the experimental observations in the positive ε_2 region. The thickness strain criterion would be quite good were it based on any data other than the uniaxial tension result (see Fig. 6b). Thus while both failure criterion may be used to describe the behavior of the basal texture, high R-value sheet (Fig. 6a), neither criterion describes fully the fracture behavior of the basal-transverse sheet.

SUMMARY

This study has examined the punch stretching behavior of strongly textured Ti-6Aℓ-4V sheet with R-values ranging from 0.5 to 12 but with relatively constant strain and strain rate hardening exponents (n = 0.5 - 0.6 and m = .012 - .016). A comparison of the experimentally determined forming limit and fracture limit curves, which lie very close to each other, shows that difficult through-thickness slip and a high R-value enhances the limit strains and fracture strains in the negative minor strain region, especially at or near uniaxial tension. In contrast, a high R-value has little effect on behavior near plane strain stretching. The intervention of fracture prior to localized necking in this study precludes a direct determination of the effect of plastic anisotropy on localized necking in the biaxial stretch forming region of the FLD. However, available data on CP Ti and Ti-6-4 suggests that increasing the R-value decreases the limit strain when the minor strain is positive. For the most part, the effects of plastic anisotropy on the localized necking as well as the fracture behavior can be understood in terms of critical thickness strain criteria. The observed fracture behavior can also be explained in terms of a distinctly different, stress-based fracture criteria.

ACKNOWLEDGEMENTS

Table I. Mechanical properties of textured Ti alloy
sheet deformed at room temperature and a
strain rate of $\sim 10^{-4}s^{-1}$.

Materials	Texture	Orientation	σ_y (MPA)	n	m	R
Ti-6Aℓ-4V	Basal texture	RD,45°,TD	780	.052	.016	12
Ti-6Aℓ-4V	Basal-transverse texture	RD	720	.065	.013	0.5
		25°	720	.052	.012	0.7
		45°	760	.039	.014	2.1
		75°	890	.036	.010	1.3
		TD	875	.047	.012	1.0
Ti-6Aℓ-4V[7]	Weak texture		965	.065	.016	0.6-1.0
Ti-5Aℓ-2.5Sn	Basal texture	RD,TD	690	.066	.014	12
CP-Ti[14]	CP texture	RD,TD	395,420	.136	.023	3.7

REFERENCES

1. S. S. Hecker in _Formability, Analysis, Modeling, and Experimentation_, p. 150, The Met. Soc. of AIME, New York, 1978.

2. P. B. Mellor, Int. Met. Rev., 1981, vol. 26, p. 1.

3. A. N. Bramley and P. B. Mellor, Int. J. Mech. Sci., 1966, vol. 8, p. 101.

4. R. M. S. Horta, W. T. Roberts, and D. V. Wilson, Int. J. Mech. Sci., 1970, vol. 12, p. 231.

5. J. Woodthrope and R. Pearce, Sheet Met. Ind., 1969, vol. 46, p. 1061.

6. K. S. Chan and D. A. Koss, Technical Report No. 19, Office of Naval Research Contract N00014-76-C-0037, NR 031-756, April, 1981.

7. K. Okazaki, M. Kagawa, and H. Conrad in _Titanium '80_, p. 863, The Met. Soc. of AIME, New York, 1980.

8. A. J. Hatch, Trans. AIME, 1965, vol. 233, p. 44.

9. D. Lee and W. Backofen, Trans. AIME, 1966, vol. 236, p. 1696.

10. M. A. W. Lowden and W. B. Hutchinson, Met. Trans. A, 1975, vol. 6A, p. 441.

11. R. A. Fishburn, W. T. Roberts, and D. V. Wilson, Met. Tech., 1976, vol. 3, p. 310.

12. F. Larson and A. Zurkadas, _Properties of Textured Titanium Alloys_, Report MCIC-74-20, 1974, Battelle Columbus Lab., Columbus, OH, p. 1.

13. S. S. Hecker, Sheet Metal Ind., 1975, vol. 52, p. 671.

14. R. J. Bourcier and D. A. Koss, Scripta Met. (in print).

15. Z. Marciniak and K. Kuczynski, Int. J. Mech. Sci., 1967, vol. 9, p. 609.

16. K. S. Chan, D. A. Koss, and A. K. Ghosh, unpublished research.

17. Z. Marciniak in _Mechanics of Sheet Metal Forming_, p. 215, Plenum Press, New York, 1978.

18. K. W. Neale and E. Chater, Int. J. Mech. Sci., 1980, vol. 22, p. 563.

19. Z. Marciniak, K. Kuczynski and T. Pokora, Int. J. Mech. Sci., 1973, vol. 15, p. 780.

20. R. Sowerby and J. L. Duncan, Int. J. Mech. Sci., 1973, vol. 15, p. 217.

21. N. M. Wang and M. L. Wenner in _Mechanics of Sheet Metal Forming_, p. 367, Plenum Press, New York, 1978.

22. G. LeRoy and D. Embury in _Formability_, p. 183, The Met. Soc. of AIME, New York, 1978.

23. A. K. Ghosh, Met. Trans. A, 1976, vol. 7A, p. 523.

24. R. J. Bourcier, R. E. Smelser, O. Richmond, and D. A. Koss, to be presented at the Ninth U.S. National Congress of Applied Mechanics, Cornell Univ., June 21-25, 1982.